Continuous Synthesis of Palladium Nanorods in Oxidative Segmented Flow

Victor Sebastian, Soubir Basak, and Klavs F. Jensen
Dept. of Chemical Engineering, Massachusetts Inst. of Technology, 77 Massachusetts Avenue, Cambridge, MA 02139

DOI 10.1002/aic.15029
Published online September 23, 2015 in Wiley Online Library (wileyonlinelibrary.com)

Laminar and segmented flow methods are presented for producing Pd rod-shaped nanostructures from Na_2PdCl_4 in mixtures of water, ethylene glycol, polyvinyl pyrrolidone, and KBr. Synthesis in laminar flow produced an evolution from Pd nanoparticles to short nanorods with residence time. Use of air as the segmentation gas tuned the oxidative environment promoting anisotropic growth of Pd. Moreover, the elevated temperatures (160°C and 190°C) and pressure (0.8 MPa) reduced the synthesis time from hours for most batch systems to 2 min. The ratio of polyol and Pd precursor metal flow streams controlled the anisotropic growth, obtaining nanorods with a diameter approximately 4 nm and an aspect ratio up to 6. Nanorods were single crystal with the {100} lattice spacing of fcc structure, and without any dislocation, stacking fault, or twin defects. The resulting Pd nanorods had high activity at moderate temperature (40°C) and pressure (0.2 MPa) in the catalytic hydrogenation of styrene. © 2015 American Institute of Chemical Engineers *AIChE J*, 62: 373–380, 2016

Keywords: palladium nanorods, oxidative etching, microfluidic reactor, segmented flow, hydrogenation reaction

Introduction

One-dimensional metal nanostructures, such as nanowires and nanorods, have attracted much research attention for their unique optical, electronic, magnetic, catalytic, and sensing properties.[1–6] Methods for synthesizing nanorods with controllable aspect ratio have used multistep seeding approaches[7] as well as electrochemical and membrane-template syntheses.[8] Herein, we present the use of a micro-fluidic reactor as a versatile tool for continuous synthesis of anisotropic palladium nanorods at short residence times (minutes).

Micro-fluidic reactors are an attractive technology with their ability to rapidly mix reagents, provide homogeneous reaction environments (temperature, pressure and concentration), continuously vary reaction conditions, and add reagents at precise time and location during a chemical reaction. In the last years, there has been an intense activity in the application of this technology to the synthesis of high quality nanomaterials.[9,10] Nanocrystalline colloids of a wide variety of nanomaterials have been synthesized, including simple nanostructures such as Cu,[11] Au,[12] CdS,[13] TiO_2,[14] SiO_2,[15] MOFs,[16] and complex nanostructures with a core-shell morphology such as SiO_2/Au,[17] CdSe/ZnSe/ZnS,[18] or even hollow nanostructures.[19] However, the production of nanostructures under a shape control process in which kinetic control prevails over thermodynamic factors,[20] is practically unexplored because of the great number of variables affecting the growth process of anisotropic nanocrystals (kinetics, synthesis conditions, ligands, additives).[21] The properties of anisotropic nanostructures (Au[22], Ag[23], Iron oxides[24]) are highly sensitive to the morphology, and thus, realizing them requires exquisite control during the synthesis process. Although microfluidic processing technology is promising, it suffers from two principal problems: propensity of fouling after extended operation and velocity dispersion.[25] Segmented flow microfluidic reactors hinder those drawbacks by introducing an immiscible fluid (gas or liquid), causing the reaction phase split into discrete drops. This technique has been successfully applied in the production of a wide range of nanoparticles such as Au,[19,22,26] Pd,[27] quantum dots,[28,29] iron oxides,[24,30] and microporous nanomaterials.[16,31]

Palladium is chosen in this work for its catalytic activity in hydrogenation and organic coupling reactions.[1,32,33] Shape selective synthesis of Pd nanoparticles is particularly of interest as the catalytic activity of nanoparticles depends on the relative distribution of facets, edges, and corners.[34] Xiong et al.[35] used a polyol/water system in the presence of polyvinyl pyrrolidone and potassium bromide (KBr) to form nanorods and nanobars. They demonstrated the importance of Br^- anions to promote the formation of {100} and {110} facets and the oxidative etching to initiate the preferential growth. Huang et al.[36] also reported high yield of Pd nanorods in 8 h synthesis. Kim et al.[27] realized bar shape nanoparticles using pinched PTFE tubing to promote efficient mixing of the growth precursors. Nevertheless, the anisotropic growth achieved was limited (average aspect ratio ~1.2).

We report a continuous segmented flow microfluidic approach to synthesize Pd nanorods. The use of air as the

Correspondence concerning this article should be addressed to K. F. Jensen at kfjensen@mit.edu.

Current address of Victor Sebastian: Dept. of Chemical Engineering, Aragon Institute of Nanoscience (INA), University of Zaragoza, 50018, Zaragoza, Spain.

Current address of Soubir Basak: SunEdison Semiconductor, Crystal R&D, 501 Pearl Drive, St. Peters, MO, 63376.

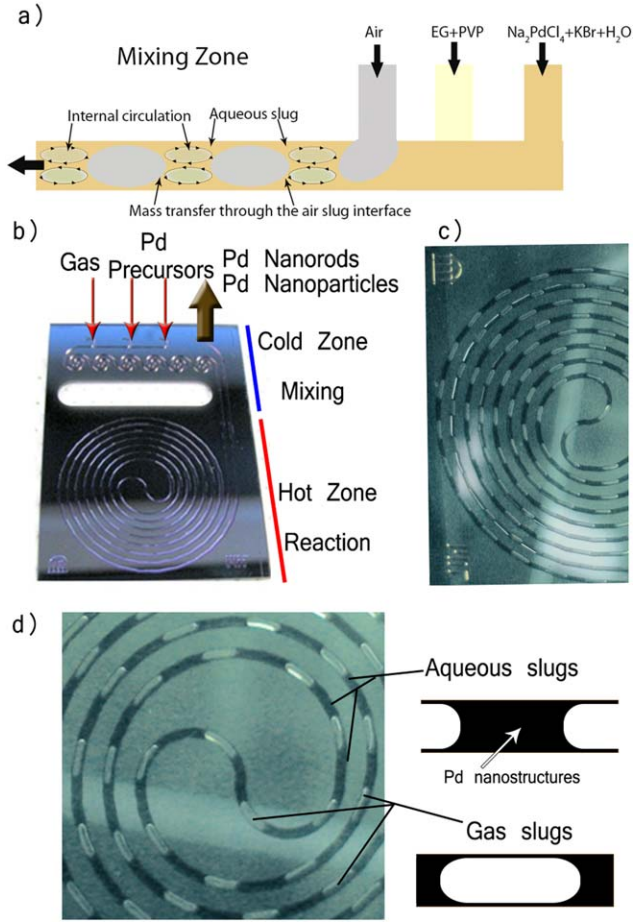

Figure 1. (a) Schematic of the segmented flow generation in the mixing zone of a hydrophilic microfluidic reactor. (b) Spiral microreactor with 400 μL channel width and depth, and 100 μL volume used for the synthesis of Pd nanorods. (c) Liquid flow segmentation by the gas phase. (d) Detail of the gas/aqueous segments generated at 160°C and a residence time of 2 min. The black segments contain Pd nanoparticles.

[Color figure can be viewed in the online issue, which is available at wileyonlinelibrary.com.]

segmentation gas provides the oxidative environment promoting the anisotropic growth of Pd in the polyol method.[20] Moreover, the use of elevated temperatures and pressure reduces the synthesis time from hours to 2 min. The resulting Pd nanorods are shown to have high activity in the catalytic hydrogenation of styrene.

Experimental Section

Reagents

Sodium Palladium(II) Chloride (Na_2PdCl_4, Aldrich); KBr (Aldrich); Polyvinyl Pyrrololidone (PVP; Aldrich MW = 55000); *N*,*N*-dimethylformamide (DMF; EMD chemicals); Ethylene Glycol (EG, Aldrich); Styrene (Aldrich,99.9%); Pd supported on activated carbon (Aldrich, 1% wt.). All reagents were used as received.

Microfluidic device and setup

All experiments were performed in silicon/Pyrex microreactors designed to withstand high pressure (60 MPa) and high temperature (350°C).[37] The reactor consisted of two zones (mixing and reaction) separated by a thermally isolating halo etch that allowed for a temperature gradient of over 25°C/mm[37] (Figure 1b). The chip was fabricated using conventional lithographic techniques to assure a high reproducibility in reactor replication as well as an excellent control in the design features. Meandering channels prior to the reaction zone served as passive mixers.[37] The mixing zone was maintained at room temperature to avoid a nonhomogenous nucleation during the mixing of reagents and the reaction zone (volume = 100 μL) was heated up to 180°C. A back-pressure regulator (Jasco, Model BP-1580) maintained a set pressure inside the reactor while enabling samples to be collected in a continuous mode without depressurizing the system. The pressure inside the reactor was kept constant at 0.8 MPa to assure a single liquid phase reaction process (in the absence of a segmenting gas flow). The reactant solutions were introduced through two separate inlets (Figure 1a): (1) palladium precursor (Na_2PdCl_4 + KBr + H_2O) and (2) polyol (EG and polyvinyl pyrrolidone). The palladium precursor solution consisted of KBr and Na_2PdCl_4 in ultra-pure water. The ration of Na_2PdCl_4 to H_2O was varied from 1/5000 to 1/1100 while the molar ratio of KBr to Na_2PdCl_4 was kept constant at 35. The polyol solution was prepared by dissolving PVP in EG in an EG/PVP ratio equal to 175. The streams were injected in the mixing zone by means of two high-pressure syringe pumps (ISCO-100DM). The flow rates of the two reagent streams, the temperature in the reaction zone and the residence time were modified to control the reduction rate and promote the anisotropic growth. Pd nanostructures collected at the backpressure regulator were washed with acetone to remove most of the EG, palladium precursor, and excess PVP.

For the segmented flow synthesis, a gas stream was introduced in the microfluidic reactor. The gas/liquid volume flow ratios were modified in the range of 0.8 to 3.5. Air and nitrogen were used as gas streams to explore the influence of oxidation on the Pd nanoparticle morphology. Flow segmentation promotes mixing by the recirculating flows inside the fluid segment.[38] The recirculation flow and the related enhanced mass transfer are primarily governed by the wetting characteristics of the reactor surface, physical properties of the two segmented phases, and the inlet flow rates.[18] The injection of a gas phase confines the liquid reagents into small, isolated segments (see Figures 1a, c). Accurate control of the liquid and gas stream injections was necessary to control the segmented flow velocity and the residence time. Figures 1c, d illustrate the homogenous distribution of segments achieved in the microfluidic device. The yield of nanoparticles after synthesis and before the final purification was estimated to 68%.

Characterization of synthesized Pd nanoparticles

The nanostructures were analyzed by transmission electron microscopy (TEM, Jeol Model 200CX). Aberration corrected scanning TEM (Cs-corrected STEM) images were acquired using a high angle annular dark field detector in a FEI XFEG TITAN electron microscope operated at 300 kV equipped with a CETCOR Cs-probe corrector from CEOS (LMA-INA-UNIZAR). Elemental analysis was carried out with an energy dispersive x-ray spectroscopy detector, which allowed energy dispersive x-ray analysis (EDS) during scanning.

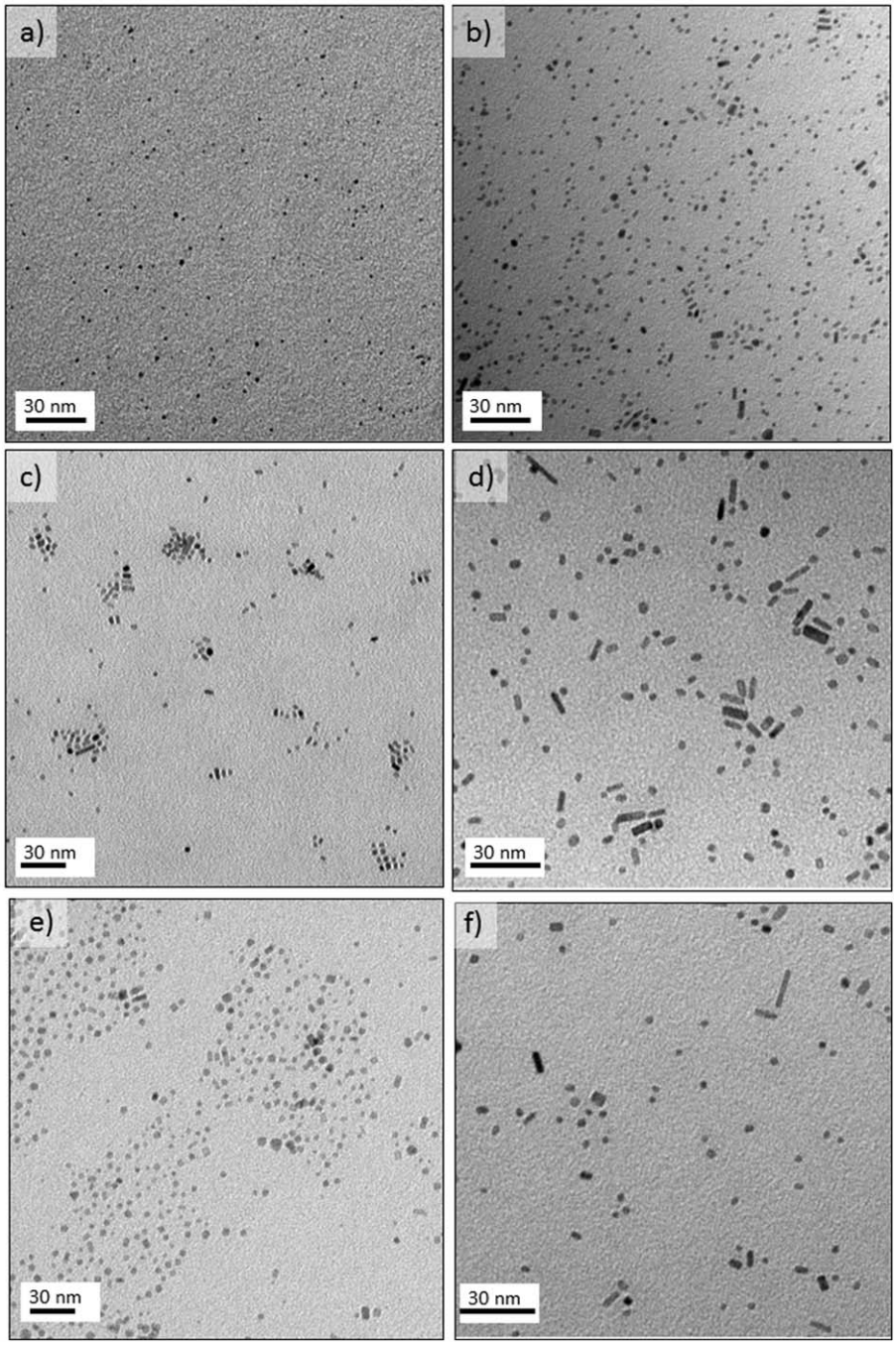

Figure 2. TEM images of Pd nanostructures obtained at different conditions Polyol/Metal = 1.8/1: (a) 10 s, 160°C; (b) 30 s, 160°C; (c) 60 s, 160°C; (d) 120 s, 160°C; (e) 120 s, 130°C; (f) 120 s, 190°C.

Hydrogenation of styrene

Catalytic hydrogenation of styrene was carried out in liquid phase using a Parr reactor. Styrene of 87 mM in DMF was reacted with 0.1 mM Pd catalyst. Total volume of the reaction mixture at the beginning of the reaction was 15 mL. Reaction temperature was maintained at 313 K using an oil bath by feedback controller. Once the temperature reached the steady state, the reactor was purged with hydrogen gas and the stirrer set at 800 rpm. Then a constant backpressure of 0.2 MPa was maintained inside the reactor with a slow bleed of hydrogen (10 ccm). Aliquot of 0.5 mL was collected at various time intervals from the sample port and analyzed with gas chromatography (Agilent, Model 6890) using FID detector. The conversion of styrene was calculated by $([\text{styrene}]_{in} - [\text{styrene}]_{out})/[\text{styrene}]_{in}$.

Results and Discussion

Laminar flow synthesis

Microfluidic synthesis in laminar flow produced an evolution from Pd nanoparticles to short nanorods as the residence time increased from 10 s to 120 s (Figures 2a–d). At 160°C and 190°C nanorods were obtained at sufficiently long residence times (120 s) (Figures 2d, f), while at lower temperatures only

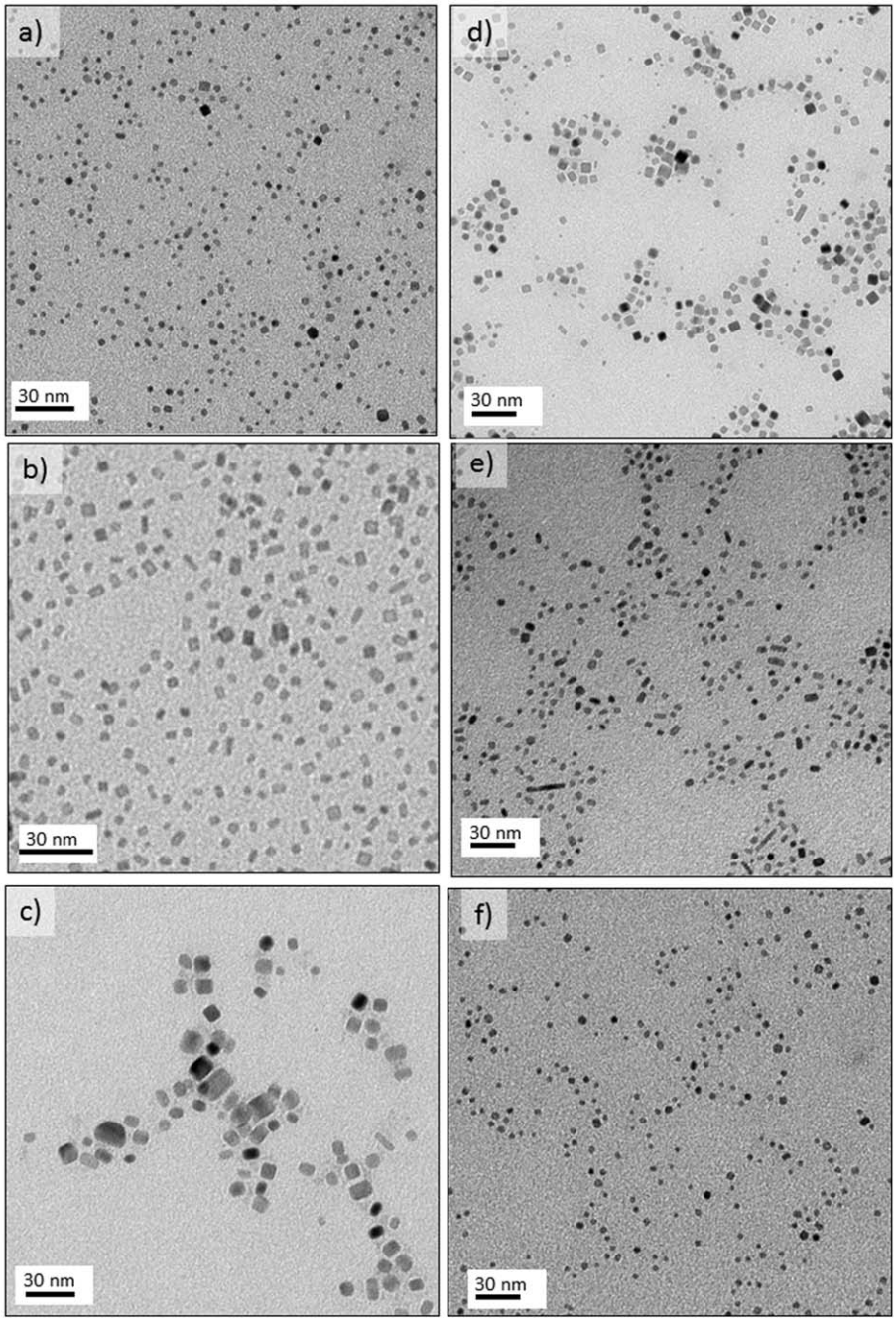

Figure 3. TEM images of Pd nanostructures obtained with different Pd/H_2O molar ratios in the metal flow at a residence time = 120 s, synthesis temperature = 160°C and Polyol/Metal = 1.8/1: (a) 1/5000, (b) 1/2200, (c) 1/1100. TEM images of Pd nanostructures obtained by oxidative etching with H_2O_2 at a residence time = 120 s, synthesis temperature = 160°C, Polyol/Metal = 1.8/1 and Pd/H_2O_2 ratio (d) 1/0.05, (e) 1/0.2, (f) 1/1.

nanoparticles formed. Oxidative etching by dissolved oxygen in the ethyleneglycol/water media and the chloride anions from the Pd precursor has been proposed as underlying the anisotropic growth of palladium nanorods.[35] The added bromide ions bind to the Pd surface preventing addition of Pd atoms from the solution. The oxidative etching removes bromide and thus activates growth. This process tends to be selective to {100} causing one facet to grow faster than other facets when there are sufficient Pd atoms available to overcome the etching reactions.

The observed results are consistent with this model. At the lower temperature (130°C), the preferential growth is not favored because the oxidative etching and the atomic additions rates are of similar magnitude.[35] At higher temperatures, the rate of generation of Pd atoms exceeds the etching and nanorods evolve with sufficient residence time. Increasing the palladium concentration induced the formation of nanocubes and nanobars with sharp edges (Figures 3a–c) consistent with batch growth observations by Tsuji et al.[39] These structures have been attributed to the role of Cl^- anions in the oxidative etching process.

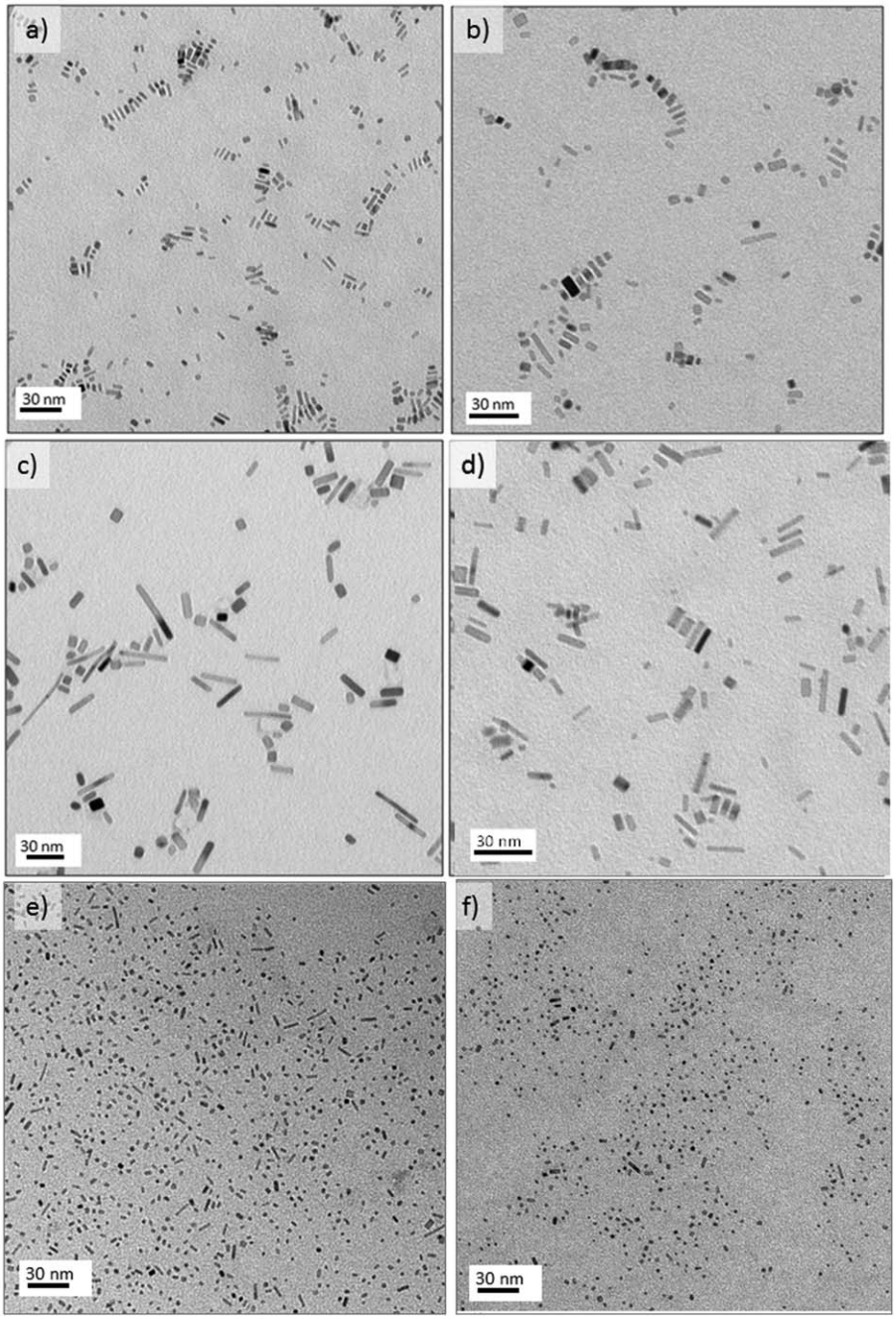

Figure 4. TEM image of Pd nanorods obtained in air segmented flow (air/liquid volume flow ratio = 3.5/1.0) at residence time of 120 s and reaction temperature 160°C, with different Po/Pd ratios: (a) 0.25, (b) 0.66, (c) 1.0, (d) 1.8, (e) 4, and (f) 9.

Air-liquid segmented flow synthesis

To control the oxidative etching that plays such a central role in the anisotropic growth, it would be useful to be able to manipulate the oxygen or chloride ion concentrations in the reaction media. An increase in Cl^- anions could lead to formation of salt crystals fouling and ultimately plugging the microfluidic reactor. Therefore, we decided to enhance the oxidative etching by two new oxygenation approaches compatible with continuous synthesis: (1) addition of hydrogen peroxide and (2) increasing the oxygen content in the synthesis media by an air-liquid segmented flow.

Addition of hydrogen peroxide increased the oxidative etching to such an extent that the growth of short Pd nanobars and cubic nanocrystals were achieved only at a Pd/H_2O_2 molar ratio as low as 0.05 (Figure 3d). Over that concentration, the dissolution of the Pd atoms occurred across the entire surface of the nanocrystals, rather than on a localized face, which promoted the growth of nanocrystals with a nearly spherical shape (Figures 3e, f). In addition, the atom etching increased with the hydrogen peroxide concentration, decreasing the size of the nanocrystals at the higher concentrations (Figure 3f).

The excellent gas-liquid mass transfer in segmented flow increased the oxygen concentration,[38] which promoted anisotropic growth and decreased the number of nanocubes in comparison with laminar flow (Figure 4). Under these synthesis conditions, the control of the three variables (bromide

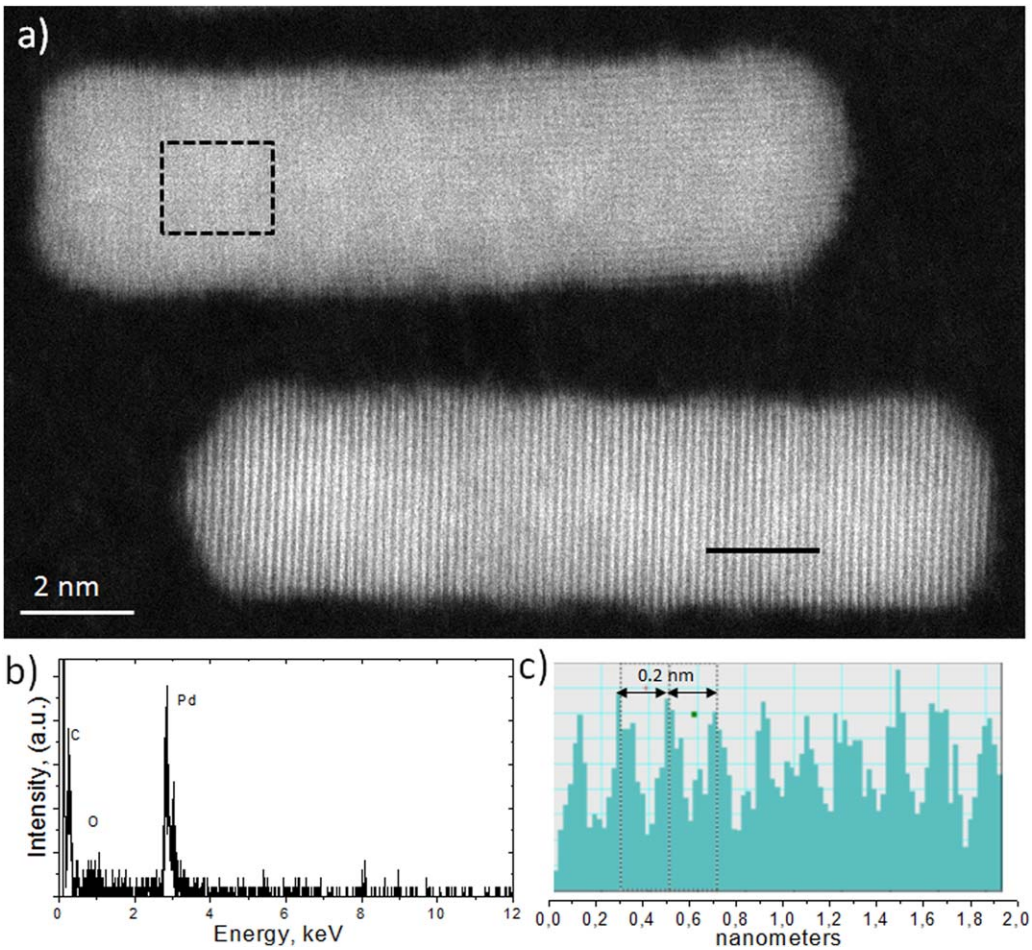

Figure 5. (a) High Magnification Cs-corrected STEM image obtained with a high-angle annular dark field (HAADF) detector of Pd nanorods obtained in air segmented flow (air/liquid = 3.5/1.0) at residence time of 120 s and reaction temperature 160°C, with a Po/Pd metal flow streams ratio of 1.8. (b) Representative EDS analysis from the selected area in (a) (square) of a single Pd nanorod. (c) Lattice fringes profile to calculate the distance between atoms.

[Color figure can be viewed in the online issue, which is available at wileyonlinelibrary.com.]

adsorption, nucleation-reduction kinetic and oxidative etching) proposed by Xiong et al.[35] made it feasible to synthesize Pd nanorods in 2 min at the elevated temperature (160°C) and pressure (0.8 MPa) in the continuous microfluidic system. In comparison, synthesis in a batch reactor required 1 h at 100°C.[35]

The ratio of polyol (Po) and Pd precursor metal flow streams (Po/Pd) controlled the anisotropic growth. The nanorod aspect

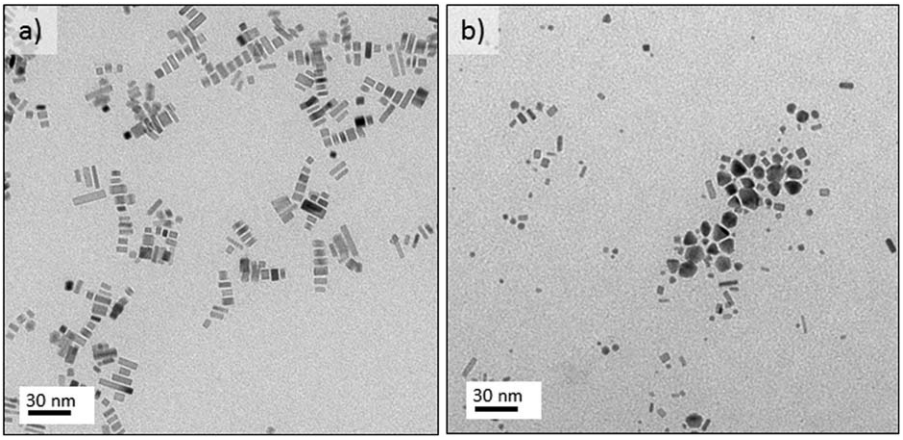

Figure 6. TEM images of the Pd nanostructures obtained with segmented flow at 160°C, 120 s residence time and Po/Pd flow stream ratio = 1.8: (a) air/liquid volume flow stream ratio = 0.8. (b) nitrogen/liquid volume flow stream ratio = 3.5.

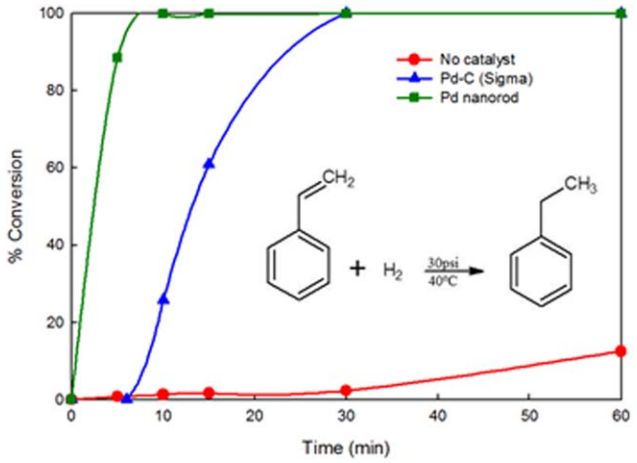

Figure 7. Conversion of styrene to ethylbenzene was plotted against reaction time at 0.2 MPa pressure and 313 K temperature for various catalyzed and uncatalyzed conditions.

[Color figure can be viewed in the online issue, which is available at wileyonlinelibrary.com.]

ratio increased from 2.5 to 6 with an increase in Po/Pd flow ratio from 0.25 to 1.8, respectively (Figures 4a–d). At a constant synthesis temperature and residence time, the reduction rate increases with EG. The resulting larger number of Pd^0 atoms facilitates the preferential growth along the *a* axis by atomic addition. Consequently, the aspect ratio of the nanorods would be expected to increase with the ratio of Po to Pd flows. However, the nanorod aspect ratio was observed to decreased when the Po/Pd flow ratio was higher than 4 (Figures 4e, f). Thus, there appears to be an optimum range of EG content to obtain anisotropic nanostructures. Low content of EG diminishes the reduction rate and the atom addition rate, while a high content of EG increase the nucleation and reduction rate such that the reduction rate of palladium ions exceeds the atom addition rate and small palladium clusters are formed by particle growth.

A high-resolution STEM image of a Pd nanorod with an aspect ratio of about 4.5 (Figure 5a) indicates that the nanorod is single crystal without any dislocation, stacking fault, or twin defects. The fringes show a period of 2.0 Å, which was consistent with the {100} lattice spacing of fcc Pd (Figure 5c).

The ratio between the air and liquid flows controls the oxidative etching. A decrease in the air to liquid ratio reduces the gas slug length. The slug length is an important hydrodynamic parameter, along with the slip velocity. Both parameters have a significant effect on gas-liquid mass transfer[38] and consequently the oxygen supply to the liquid phase. As a result, the oxidative etching rate is low and the anisotropic growth is less favored; under such conditions nanorods with a low aspect ratio are produced (Figure 6a). The gas-liquid segmented flow also enhances the mixing and eliminates the axial dispersion, which make this flow pattern an efficient approach for nanostructures synthesis.[15] When air is replaced by nitrogen, anisotropic growth does not occur (Figure 6b). The most striking differences observed, with respect to the approach reported by Kim et al.,[27] are that the Pd nanostructures shape and size can effectively be tuned by the modification of the composition of gas and liquid slugs to promote the growth of anisotropic Pd nanostructures with high-aspect ratio (Figures 4c, d).

Hydrogenation of styrene

To evaluate the catalytic activity of the synthesized Pd nanorods in hydrogenation, they were characterized in the catalytic hydrogenation of styrene and the results benchmarked to those with commercial Pd catalyst from Sigma. The Pd nanorods showed enhanced catalytic activity and no induction time toward the hydrogenation of styrene under similar condition (Figure 7). The measure catalytic activity was also compared with reported catalytic hydrogenation of styrene at different reaction conditions (Table 1).[40–43] Under moderate temperature (40°C) and pressure (0.2 MPa) Pd nanorods synthesized by microfluidic reactor process show high turnover number (840) and frequency (6297 h^{-1}) calculated based on the final reaction conversion.

Conclusion

We have shown that microfluidic systems facilitate fast screening of reagent mixtures and reaction conditions for synthesis of anisotropic Pd nanostructures. Moreover, introduction of air as a segmentation gas improved dispersion characteristics and allowed balancing of etching and addition processes to realize high aspect ratio Pd nanorods. Furthermore, the elevated temperatures (160–190°C) and pressure (0.8 MPa) used in the microfluidic reduced the synthesis time from hours for most batch systems to 2 min. Finally as a demonstration, the resulting Pd nanorods displayed high activity at

Table 1. Comparison of Catalyst Performance for Hydrogenation of Styrene Under Various Reaction Conditions

Catalyst	Pressure (MPa)	Temperature (°C)	Solvent	Reaction Time (min)	% Conversion	% Yield	Turnover Number	Turnover Frequency (hr)
Without catalyst*	0.2	40	DMF	60	12.5	2.9	*x*	*x*
Pd-C (Sigma)*	0.2	40	DMF	30	100	88.6	771	1542
Pd nanorod*	0.2	40	DMF	8	100	96.5	840	6297
$Ru_3(CO)_{12}$/ PETPP[24]	1.0	90	Toluene	180	100	99.5	995	332
PdCl-673[22]	1.0	80	Toluene	40	100	98	25480	38220
Pd-C[23]	0.2	30	Dodecane	60	45	95	679	679
Perfluoroalkylated BINAP–Rh(I) complexes[21]	1.0	50	Supercritical CO_2	180	100	100	500	167

*In this study.

moderate temperature (40°C) and pressure (0.2 MPa) in the catalytic hydrogenation of styrene.

Acknowledgments

Authors acknowledge U.S. National Science Foundation (CHE-0714189) for funding this research. V.S. acknowledges the support of the Fulbright Commission and the Ministry of Education in Spain (Programa Nacional de Movilidad de Recursos Humanos del Plan Nacional de I+D+I 2008-2011), as well as People Program (CIG-Marie Curie Actions, REA grant agreement no. 321642) to develop this research.

Literature Cited

1. Xia YN, Yang PD, Sun YG, Wu YY, Mayers B, Gates B, Yin YD, Kim F, Yan YQ. One-dimensional nanostructures: synthesis, characterization, and applications. *Adv Mater*. 2003;15:353–389.
2. Zhai TY, Fang XS, Liao MY, Xu XJ, Zeng HB, Yoshio B, Golberg D. A comprehensive review of one-dimensional metal-oxide nanostructure photodetectors. *Sensors*. 2009;9:6504–6529.
3. Ahn JR, Kim YJ, Lee HS, Hwang CC, Kim BS, Yeom HW. Electronic nature of one-dimensional noble-metal nanowires on the Si(5512) surface. *Phys Rev B*. 2002;66, number of publication 153403.
4. Sun Y, Zhang FY, Xu L, Yin ZL, Song XY. Roughness-controlled copper nanowires and Cu nanowires-Ag heterostructures: synthesis and their enhanced catalysis. *J Mater Chem A*. 2014;2:18583–18592.
5. Dorantes-Davila J, Pastor GM. Magnetic anisotropy of one-dimensional nanostructures of transition metals. *Phys Rev Lett*. 1998;81:208–211.
6. Sebastian V, Lee SK, Zhou C, Kraus MF, Fujimoto JG, Jensen KF. One-step continuous synthesis of biocompatible gold nanorods for optical coherence tomography. *Chem Commun*. 2012;48:6654–6656.
7. Nikoobakht B, Wang ZL, El-Sayed MA. Self-assembly of gold nanorods. *J Phys Chem B*. 2000;104:8635–8640.
8. Yu YY, Chang SS, Lee CL, Wang CRC. Gold nanorods: electrochemical synthesis and optical properties. *J Phys Chem B*.1997;101:6661–6664.
9. Marre S, Jensen KF. Synthesis of micro and nanostructures in microfluidic systems. *Chem Soc Rev*. 2010;39:1183–1202.
10. Krishna KS, Li YH, Li SN, Kumar CSSR. Lab-on-a-chip synthesis of inorganic nanomaterials and quantum dots for biomedical applications. *Adv Drug Deliver Rev*. 2013;65:1470–1495.
11. Song YJ, Doomes EE, Prindle J, Tittsworth R, Hormes J, Kumar CSSR. Investigations into sulfobetaine-stabilized cu nanoparticle formation: toward development of a microfluidic synthesis. *J Phys Chem B*. 2005;109:9330–9338.
12. Wagner J, Kohler JM. Continuous synthesis of gold nanoparticles in a microreactor. *Nano Lett*. 2005;5:685–691.
13. Hung LH, Choi KM, Tseng WY, Tan YC, Shea KJ, Lee AP. Alternating droplet generation and controlled dynamic droplet fusion in microfluidic device for CdS nanoparticle synthesis. *Lab Chip*. 2006; 6:174–178.
14. Cottam BF, Krishnadasan S, deMello AJ, deMello JC, Shaffer MSP. Accelerated synthesis of titanium oxide nanostructures using microfluidic chips. *Lab Chip*. 2007;7:167–169.
15. Khan SA, Gunther A, Schmidt MA, Jensen KF. Microfluidic synthesis of colloidal silica. *Langmuir*. 2004;20:8604–8611.
16. Paseta L, Seoane B, Julve D, Sebastian V, Tellez C, Coronas J. Accelerating the controlled synthesis of metal-organic frameworks by a microfluidic approach: a nanoliter continuous reactor. *ACS Appl Mater Interfaces*. 2013;5:9405–9410.
17. Gomez L, Arruebo M, Sebastian V, Gutierrez L, Santamaria J. Facile synthesis of SiO2-Au nanoshells in a three-stage microfluidic system. *J Mater Chem*. 2012;22:21420–21425.
18. Lee CG, Uehara M, Nakamura H, Maeda H. High temperature preparation of core and core/shell composite nanocrystals in a multiphase microreactor. *J Chem Eng Jpn*. 2008;41:644–648.
19. Gomez L, Sebastian V, Irusta S, Ibarra A, Arruebo M, Santamaria J. Scaled-up production of plasmonic nanoparticles using microfluidics: from metal precursors to functionalized and sterilized nanoparticles. *Lab Chip*. 2014;14:325–332.
20. Xiong YJ, Xia YN. Shape-controlled synthesis of metal nanostructures: the case of palladium. *Adv Mater*. 2007;19:3385–3391.
21. Sebastian V, Arruebo M, Santamaria J. Reaction engineering strategies for the production of inorganic nanomaterials. *Small*. 2014;10: 835–853.
22. Duraiswamy S, Khan SA. Droplet-based microfluidic synthesis of anisotropic metal nanocrystals. *Small*. 2009;5:2828–2834.
23. Knauer A, Kohler JM. Screening of multiparameter spaces for silver nanoprism synthesis by microsegmented flow technique. *Chem-Ing-Tech*. 2013;85:467–475.
24. Larrea A, Sebastian V, Ibarra A, Arruebo M, Santamaria J. Gas slug microfluidics: a unique tool for ultrafast, highly controlled growth of iron oxide nanostructures. *Chem Mater*. 2015;27:4254–4260.
25. Nightingale AM, deMello JC. Segmented flow reactors for nanocrystal synthesis. *Adv Mater*. 2013;25:1813–1821.
26. Cabeza VS, Kuhn S, Kulkarni AA, Jensen KF. Size-controlled flow synthesis of gold nanoparticles using a segmented flow microfluidic platform. *Langmuir*. 2012;28:7007–7013.
27. Kim YH, Zhang L, Yu T, Jin M, Qin D, Xia Y. Droplet-based microreactors for continuous production of palladium nanocrystals with controlled sizes and shapes. *Small*. 2013;9:3462–3467.
28. Nightingale AM, Krishnadasan SH, Berhanu D, Niu X, Drury C, McIntyre CR, Valsami-Jonesb CE, deMello JC. A stable droplet reactor for high temperature nanocrystal synthesis. *Lab Chip*. 2011; 11:1221–1227.
29. Baek J, Allen PM, Bawendi MG, Jensen KF. Investigation of indium phosphide nanocrystal synthesis using a high-temperature and high-pressure continuous flow microreactor. *Angew Chem Int Ed*. 2011; 50:627–630.
30. Kumar K, Nightingale AM, Krishnadasan SH, Kamaly N, Wylenzinska-Arridge M, Zeissler K, Branford WR, Ware E, deMello AJ, deMello JC. Direct synthesis of dextran-coated superparamagnetic iron oxide nanoparticles in a capillary-based droplet reactor. *J Mater Chem*. 2012;22:4704–4708.
31. Hoang PH, Park H, Kim DP. Ultrafast and continuous synthesis of unaccommodating inorganic nanomaterials in droplet- and ionic liquid-assisted microfluidic system. *J Am Chem Soc*. 2011;133: 14765–14770.
32. Xia YN, Xiong YJ, Lim B, Skrabalak SE. Shape-controlled synthesis of metal nanocrystals: simple chemistry meets complex physics? *Angew Chem Int Ed*. 2009;48:60–103.
33. Calo V, Nacci A, Monopoli A, Montingelli F. Pd nanoparticles as efficient catalysts for Suzuki and Stille coupling reactions of aryl halides in ionic liquids. *J Org Chem*. 2005;70:6040–6044.
34. Cheong SS, Watt JD, Tilley RD. Shape control of platinum and palladium nanoparticles for catalysis. *Nanoscale*. 2010;2:2045–2053.
35. Xiong YJ, Cai HG, Wiley BJ, Wang JG, Kim MJ, Xia YN. Synthesis and mechanistic study of palladium nanobars and nanorods. *J Am Chem Soc*. 2007;129:3665–3675.
36. Huang XQ, Zheng NF. One-pot, high-yield synthesis of 5-fold twinned Pd nanowires and nanorods. *J Am Chem Soc*. 2009;131: 4602–4603.
37. Marre S, Adamo A, Basak S, Aymonier C, Jensen KF. Design and packaging of microreactors for high pressure and high temperature applications. *Ind Eng Chem Res*. 2010;49:11310–11320.
38. Gunther A, Khan SA, Thalmann M, Trachsel F, Jensen KF. Transport and reaction in microscale segmented gas-liquid flow. *Lab Chip*. 2004;4:278–286.
39. Tsuji M, Matsumoto K, Jiang P, Matsuo R, Tang XL, Karnarudin KSN. Roles of Pt seeds and chloride anions in the preparation of silver nanorods and nanowires by microwave-polyol method. *Colloids Surf A*. 2008;316:266–277.
40. Altinel H, Avsar G, Yilmaz MK, Guzel B. New perfluorinated rhodium-BINAP catalysts and hydrogenation of styrene in supercritical CO2. *J Supercrit Fluid*. 2009;51:202–208.
41. Badano J, Lederhos C, Quiroga M, L'Argentiere P, Coloma-Pascual F. Low metal loading catalysts used for the selective hydrogenation of styrene. *Quim Nova*. 2010;33:48–51.
42. Jackson SD, Shaw LA. The liquid-phase hydrogenation of phenyl acetylene and styrene on a palladium/carbon catalyst. *Appl Catal A-Gen*. 1996;134:91–99.
43. Wang YH, Wu XW, Cheng F, Jin ZL. Thermoregulated phase-separable Ru3(CO)12/PETPP complex catalyst for hydrogenation of styrene. *Chin Chem Lett*. 2002;13:1011–1012.

Manuscript received July 5, 2015, and revision received Aug. 28, 2015.